Electric Power System Studies for a Multi-MW PV Farm and Large Rural Community with Net Zero Energy and Microgrid Capabilities

Evan S. Jones
Student Member, IEEE
SPARK Laboratory
ECE Dept.
University of Kentucky
Lexington, KY, US
SEvanJones@uky.edu

Oluwaseun M. Akeyo
Student Member, IEEE
SPARK Laboratory
ECE Dept.
University of Kentucky
Lexington, KY, US
m.akeyo@uky.edu

Keith Waters, P.E.
Senior Member, IEEE
Schneider Electric
Lexington, KY, US
keith.waters@se.com

Dan M. Ionel
Fellow, IEEE
SPARK Laboratory
ECE Dept.
University of Kentucky
Lexington, KY, US
dan.ionel@ieee.org

***Abstract*— Solar photovoltaic (PV) systems are currently being deployed at an accelerated rate because of their cost-competitiveness and environmental benefits, which make them a prime candidate for local renewable energy generation in communities. Microgrids can coordinate different distributed energy resources (DERs), such as PV systems, while islanded or by drawing power from the utility while in grid-connected mode. An islanding option is also important for resilience and grid fault mitigation, even if other DERs are not present within the system. This paper studies the potential benefits that a multi-MW utility-scale PV farm may yield for a large rural community when installed within a grid-connected microgrid structure. The PV system was optimally sized based on net present cost (NPC) with a net zero energy (NZE) goal. With local solar PV generation and a connection to transmit overgeneration to the grid, the community can be NZE by having a PV farm power rating that is much greater than the peak load demand. This may lead to cases of increased transient severity during mode transitions and may require substantial curtailment of PV. A control scheme is proposed to smooth system transients that result from the switching between the two modes of operation in order to avoid system damage or unreliable load service.**

***Index Terms*—Net Zero Energy, Microgrid, Renewable, Grid-Connected, Solar PV.**

I. Introduction

Solar photovoltaic (PV) installations experience accelerated deployment growth due to competitive economic cost trends and beneficial environmental impacts, including the elimination of carbon emissions during generation. Furthermore, when combined with other distributed energy resources (DER) and advanced technologies, such as microgrids and battery energy storage systems (BESS), solar PV may contribute to improving the availability and reliability of the electric power supply [1].

This paper presents a study into the potential benefits provided by a multi-MW utility size PV farm installed near a large rural community. It includes calculations for net zero energy (NZE) balance over a year and simulations of special controls that allow operation both in grid-connected mode, as well as in microgrid islanded mode. The study considers a rating of 175MW corresponding to a PV installation covering approximately 800 acres in Southern Kentucky in the vicinity of Glasgow, KY, a community with more than 7,000 homes, which includes one of the largest US rural demonstrators of smart grid implementation, and for which weather and electric load data is available [2].

The smoothing of system transients caused by the switching operation in between grid-connected and islanded microgrid is very important for the stability and reliability of the system. Voltage source converters have been used in order to maintain voltage and frequency with a fuzzy logic controller designed specifically for islanded operation to accommodate for system non-linearity and to limit transient effects [3]. A current control method has also been employed for grid-connected mode with an inverter voltage control based on a phase locked loop (PLL) for islanding [4]. In this case, the PLL had synchronized the phases of the inverter and the grid, but other techniques have employed a second order sequence based frequency locked loop for grid synchronization [5]. Multi-droop control strategies to mitigate voltage and frequency disturbances during mode transitions were developed and studied through simulation models [6]. Droop methods have also been used as a control scheme for industrial PV microgrids where a PLL was employed to smooth mode transition [7].

Transfer strategies intended to provide seamless transitions have been simulated in PSCAD/EMTDC for microgrids with a variety of DERs [8]. Other research has used MATLAB/Simulink to simulate control strategies with more of a focus on BESS and DER performance as well as different grid synchronization requirements [9], [10]. In the current paper, the microgrid structure is simulated so that the system transients may be analyzed and improved.

II. System Component Sizing

The component sizing for the Glasgow, KY electric power load was performed with the HOMER Pro microgrid optimization software [11]. HOMER considers cost and power ratings of components as well as load profile, local weather, and project lifetime. All ”winning” solutions produced by the

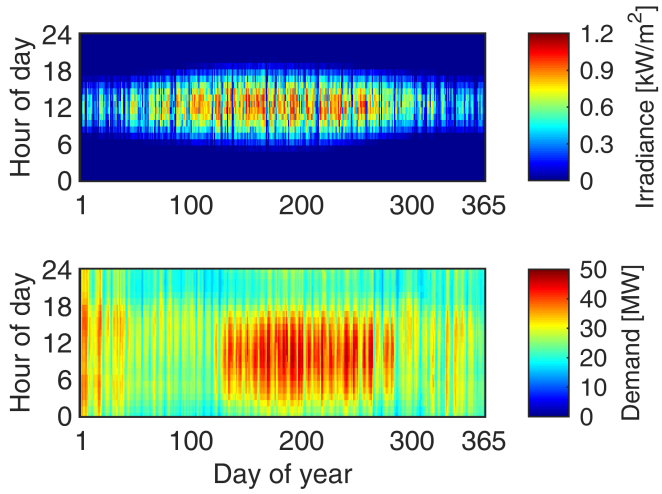

Figure 1. Annual irradiance and electric demand for Glasgow, KY in 2018. They follow a similar seasonal pattern, but are not as aligned throughout the day. Peak irradiance occurs in the evening when the sun is most direct, and peak demand is later in the afternoon as people return home.

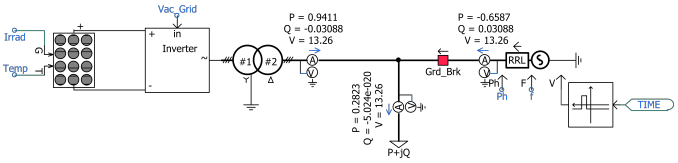

Figure 2. Electric circuit diagram of the proposed microgrid in the PSCAD/EMTDC software. This system includes a PV array, three-phase inverter, a three-phase voltage source as the grid, and a fixed load that is representative of the average demand in Glasgow, KY.

optimizer were made to be NZE by constraining the annual energy grid purchases to 0kWh. The software's optimization algorithm regards the net present cost (NPC) of the entire system as the most important value to minimize. NPC is defined by:

$$NPC = (C_c + C_r + C_{O\&M} + C_f + C_e + C_g) - (R_s + R_g), \quad (1)$$

where C_c is the capital cost, C_r the replacement cost, C_f the fuel cost, $C_{O\&M}$ the operation and maintenance cost, C_e the emissions penalties, C_g is the cost of buying power from the grid, R_s is the salvage value, and R_g the grid sales revenue.

With a relatively low grid purchase rate of only 0.0908 \$/kWh, the recommended microgrid configuration for the approximately 7,000+ home community of Glasgow, KY comprises of a large 175MW PV farm with no BESS or other DERs. The demand and irradiance measurements for Glasgow, KY in 2018 have similar seasonal patterns but are not aligned over the day (Fig. 1). The PV system will under-generate during the winter with respect to the community electric load and will over-generate in the summer. It is also confirmed that the power generation from the PV farm will experience a high degree of variability. During periods of under-generation, energy is purchased from the grid, but over-generation is sold back to the grid so that the NZE requirement of the system

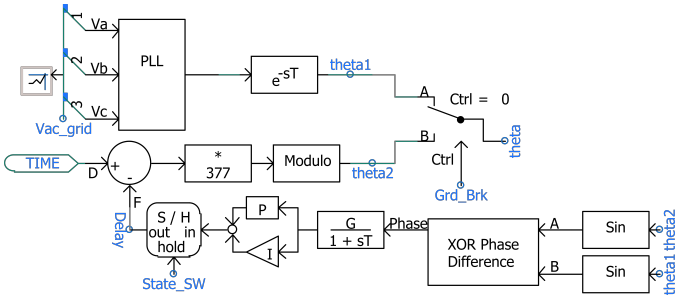

Figure 3. Processes of determining phase angle of the microgrid (theta) for both grid-connected and islanded mode. When the grid is connected, theta is extracted from the PLL. While in islanded mode, theta is generated.

may be satisfied. Since the PV system is so large compared to the demand, transients are expected to be more severe at times of typical mode transitions.

III. Microgrid System Configuration and Control

With the microgrid sizing information, a PSCAD/EMTDC model was developed to simulate the system behavior at times of mode transition (Fig. 2). The model includes a PV array, a representative average load for Glasgow, KY, and a three-phase voltage source as the utility grid. Power for these components specified in a per unit (pu) basis with 175MW, the rated power for the PV system, as the base. Other components for the model includes a breaker to enable islanding, a three-phase transformer to step-up voltage to 13.2kV, and an inverter for the PV with maximum power point tracking (MPPT).

When the proposed system is grid connected, the PV array is controlled such that it operates at the maximum power point (MPP) and the grid either absorbs or supplies the deficit power required by the microgrid. Hence, in periods during which the grid is connected, the inverter operates in MPPT mode. This ensures that the PV voltage, V_{pv}, matches its corresponding MPPT reference, V_{MPPT}. When the grid is disconnected, the PV inverter is operated in grid forming mode, where it maintains its terminal voltage and frequency at the reference values.

While in grid-connected mode, the phase angle at which the microgrid power system operates is extracted from the PLL. The PV system may be operated in grid-following (grid-connected) or grid-forming (islanded) modes and the corresponding inverter reference current components are expressed as:

$$i_d^* = \begin{cases} (V_{MPPT} - V_{pv})\left(K_{ps} + \frac{K_{is}}{s}\right) & \text{grid-connected} \\ (V_l^* - V_l)\left(K_{ps} + \frac{K_{is}}{s}\right) & \text{islanded} \end{cases} \quad (2)$$

$$i_q^* = 0, \quad (3)$$

where V_{MPPT} represents the reference MPP voltage; V_{pv}, the PV array terminal voltage; V_l, the load voltage; V_l^*, the reference load voltage; K_{ps} and K_{is}, are PI controller constants.

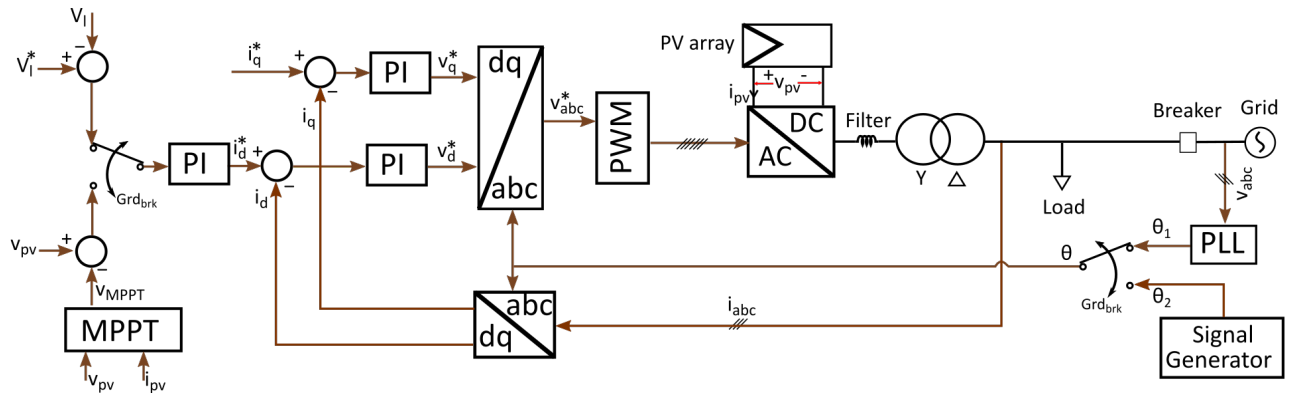

Figure 4. Control schematic for grid-connected microgrid power system with PV array.

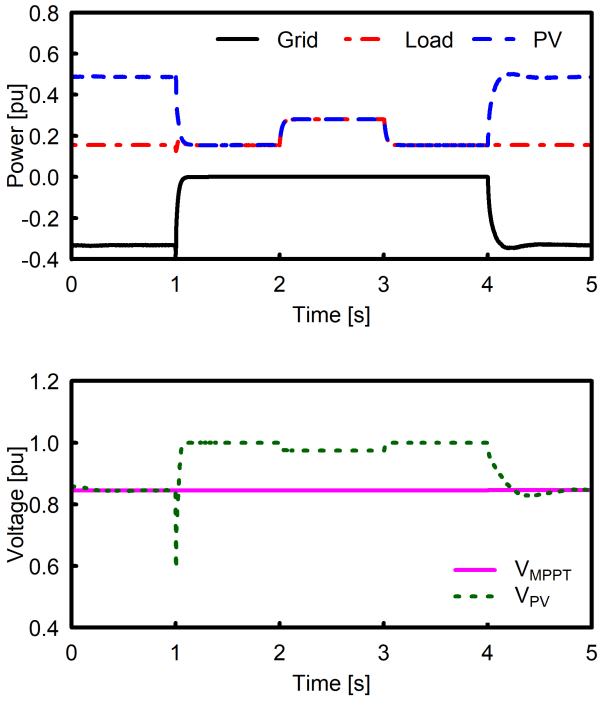

Figure 5. The real power flow of the system (a). When the grid disconnects at 1s, PV over-generation is curtailed. PV resumes operation at MPP when it is able to transmit to the grid again at 4s. Maximum power point tracker voltage for PV (b). Excess PV generation is curtailed by operating at a higher voltage than V_{MPPT} when the grid is unavailable.

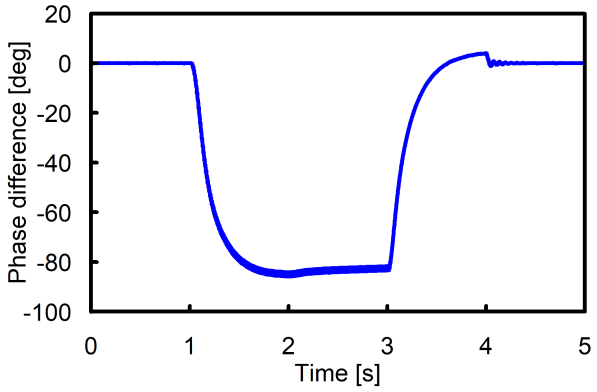

Figure 6. Phase difference between the grid voltage and the voltage of the microgrid system. Once the grid disconnects, the phase angle of the microgrid deviates from the phase angle of the utility grid. The phase angle of the microgrid system is synchronized with the grid before reconnecting.

To ensure a straightforward transition between grid connected and islanded mode, the Park transformation angle for grid forming mode is developed from a sawtooth signal generator at ω_0 (2πf) and regulated to ensure minimum phase shift with the grid angle (Fig. 3).

IV. Operation in Grid-connected and Islanded Mode

Microgrid systems may be operated in either grid-connected mode or in islanded mode. The proposed system operation was studied through the PSCAD/EMTDC simulation that confirmed the system transient response when switching between operation modes. The PV array irradiance was set to 500W/m^2, and the PV operated at maximum power point (MPP) to meet the microgrid demand and supply excess power to the grid. The grid voltage was set to zero between 1-3s simulation time to simulate grid disconnection. A control scheme was implemented in which the circuit breaker opened (Grd_{Brk} = 1) when the grid was disconnected and closed (Grd_{Brk} = 0) after a 1s delay when the grid reconnected. This method ensured a smooth transition from islanded to grid-connected mode (Fig. 5).

At 1s simulation time, when the grid was disconnected, the circuit breaker opened to island the microgrid and the PV inverter switched from grid-following to grid-forming mode to meet demand. A transient change in load can be observed at 2s simulation time, in which the demand approaches the community peak until 3s simulation time when it returns to the average value. In grid-forming mode, the PV array voltage deviated from its MPP reference to curtail its excess power as well as to regulate its terminal voltage and frequency. The Park transformation angle, θ, was also switched from

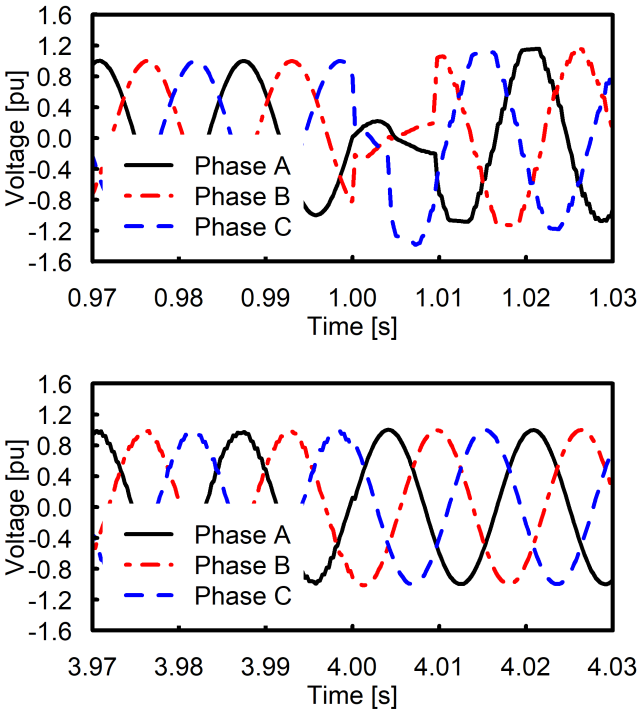

Figure 7. Voltage during transitions from grid-connected to islanded mode and then from islanded to grid-connected, respectively. System transients are more severe when disconnecting from the grid but are still confined to within only 1s.

grid-following, θ_1, to the grid-forming reference, θ_2, with minimal load voltage distortion. Alternative sources, such as a battery, is required to ensure steady power supply to load in the case that there is a solar power deficit while the grid is disconnected.

The grid voltage returned to its reference value at 3s simulation time to indicate grid availability, and the breaker delayed for 1s to allow minimum phase shift between θ_1 and θ_2 before the microgrid system and the grid were reconnected. At 4s simulation time, Grd_{Brk} closed with minimum voltage disturbance, and the inverter switched back to grid following mode to enable PV MPP operation (Fig. 7).

V. Conclusion

This paper presents a study into potential benefits of a local multi-MW utility-scale PV farm for a large rural community. For the considered weather conditions in Southern Kentucky, in order to enable the community to achieve NZE, the PV system has to be rated much larger than the peak load demand. A grid-connected microgrid structure is employed to coordinate the PV such that the load is continuously supplied with electricity, even during periods of PV under-generation, and that over-generation is transmitted to the utility grid. The microgrid may operate in either grid-connected or islanded mode for which the former allows service from the utility grid, and the latter is useful for power system reliability and fault effect mitigation. Such a relatively large amount of PV generation may increase the severity of system transients during the switching of operation modes and requires a method for smoothing, such as the one proposed and demonstrated in the paper.

With the proposed control strategy, the phase angle at which the PV inverter operates is determined differently between operation modes and can change as transitions occur. System transients are minimized and confined within one second as the grid disconnects from the microgrid since the PV inverter operates independently in grid-forming mode. As the grid is reconnected, the PV inverter is switched to grid-following mode after the phase difference is reduced and the systems are synchronized. By transitioning back to grid-connected mode at the point of minimal phase difference in this way, voltage experiences low disturbance.

Acknowledgment

The direct support of Schneider Electric and of the University of Kentucky Department of Electrical and Computer Engineering URF Program is gratefully acknowledged.

References

[1] F. Blaabjerg and D. M. Ionel, *Renewable Energy Devices and Systems with Simulations in MATLAB® and ANSYS®*. CRC Press, 2017.

[2] H. Gong, V. Rallabandi, M. L. McIntyre, and D. M. Ionel, "On the optimal energy controls for large scale residential communities including smart homes," in *2019 IEEE Energy Conversion Congress and Exposition (ECCE)*, 2019, pp. 503–507.

[3] C. Shah, M. Abolhassani, and H. Malki, "Fuzzy controlled VSC of battery storage system for seamless transition of microgrid between grid-tied and islanded mode," in *2017 International Joint Conference on Neural Networks (IJCNN)*, May 2017, pp. 3224–3227.

[4] Thanh-Vu Tran, Tae-Won Chun, Hong-Hee Lee, Heung-Geun Kim, and Eui-Cheol Nho, "Control for grid-connected and stand-alone operations of three-phase grid-connected inverter," in *2012 International Conference on Renewable Energy Research and Applications (ICRERA)*, Nov 2012, pp. 1–5.

[5] S. Kewat and B. Singh, "Grid synchronization of WEC-PV-BES based distributed generation system using robust control strategy," in *2019 IEEE Industry Applications Society Annual Meeting*, Sep. 2019, pp. 1–8.

[6] L. G. Meegahapola, D. Robinson, A. P. Agalgaonkar, S. Perera, and P. Ciufo, "Microgrids of commercial buildings: Strategies to manage mode transfer from grid connected to islanded mode," *IEEE Transactions on Sustainable Energy*, vol. 5, no. 4, pp. 1337–1347, Oct 2014.

[7] M. M. Ghahderijani, M. Castilla, A. Momeneh, R. G. Sola, and L. G. de Vicuña, "Transient analysis of PV-based industrial microgrids between grid-connected and islanded modes," in *IECON 2016 - 42nd Annual Conference of the IEEE Industrial Electronics Society*, Oct 2016, pp. 365–370.

[8] S. Wu, S. Liu, X. Chen, L. Zheng, and J. Zhu, "An intentionally seamless transfer strategy between grid-connected and islanding operation in micro-grid," in *2014 17th International Conference on Electrical Machines and Systems (ICEMS)*, Oct 2014, pp. 302–307.

[9] A. Merabet, Z. Qin, and A. M. Y. M. Ghias, "Control of simulated solar PV microgrid operating in grid-tied and islanded modes," in *IECON 2018 - 44th Annual Conference of the IEEE Industrial Electronics Society*, Oct 2018, pp. 1729–1734.

[10] B. Singh, G. Pathak, and B. K. Panigrahi, "Seamless transfer of renewable-based microgrid between utility grid and diesel generator," *IEEE Transactions on Power Electronics*, vol. 33, no. 10, pp. 8427–8437, Oct 2018.

[11] E. S. Jones, H. Gong, and D. M. Ionel, "Optimal combinations of utility level renewable generators for a net zero energy microgrid considering different utility charge rates," in *2019 8th International Conference on Renewable Energy Research and Applications (ICRERA)*, Nov 2019, pp. 1014–1017.